Poly-glutamic dendrimer-based conjugates for cancer vaccination - a computational design for targeted delivery of antigens

Moura, L. I. F.[1,2], Martinho, N. [1,2,3], Silva, L. C.[1, 4], Barata, T. S.[3], Brocchini, S.[3], Florindo, H. F.[1a], Zloh, M.[2a]

[1] Research Institute for Medicines (iMed.ULisboa), Faculty of Pharmacy, Universidade de Lisboa, Av. Professor Gama Pinto, Lisbon 1649-003, Portugal

[2] School of Life and Medical Sciences, University of Hertfordshire, College Lane, Hatfield AL10 9AB, UK

[3] Department of Pharmaceutics, UCL School of Pharmacy, 29/39 Brunswick Square, London WC1N 1AX, UK

[4] Centro de Química-Física Molecular and Institute of Nanoscience and Nanotechnology, Instituto Superior Técnico, Universidade de Lisboa, Av. Rovisco Pais, 1049-001 Lisboa, Portugal.

[a] Corresponding authors:

Professor Mire Zloh

School of Life and Medical Sciences

University of Hertfordshire

College Lane

Hatfield AL10 9AB, UK

Telephone: +44 1707 284540

Email: m.zloh@herts.ac.uk

Professor Helena F. Florindo

Research Institute for Medicines (iMed.ULisboa),

Faculty of Pharmacy

Universidade de Lisboa

Avenida Professor Gama Pinto

1649-003 Lisbon – Portugal

Telephone: +351 217946400

Email: hflorindo@ff.ulisboa.pt

ABSTRACT

Computational techniques are useful to predict interaction models and molecular properties for the design of drug delivery systems, such as dendrimers. Dendrimers are hyperbranched macromolecules with repetitive building blocks, defined architecture and functionality. This work evaluated the impact of surface modifications of mannosamine-conjugated multifunctional poly (glutamic acid) (PG)-dendrimers as nanocarriers of the tumor associated antigens (TAA) MART-1, gp100:44 and gp100:209. Their potential to target antigen presenting cells through molecular interactions with mannose receptor (MR1) to promote an efficient and selective antitumor immunotherapeutic effect was also evaluated.

Molecular dynamics (MD) simulations and docking studies were performed. Results showed that nitrobenzoxadiazole (NBD)-PG-G4-dendrimer displayed 64 carboxylic groups, however the frontier molecular orbital theory study has indicated that only 32 of those carboxylic groups present on the backbone were available to form covalent bonds with either mannosamine or TAA. No differences in the gap energy of HOMO of conjugated NBD-PG-G4-dendrimer and LUMO of conjugating agents were observed while increasing conjugation loading. When the number of mannosamines conjugated to dendrimer was increased from 16 to 32, the conjugated dendrimer interacted with the receptor with higher affinity. However, due to absence of available carboxylic end groups of backbone chain for further conjugation in a dendrimer with 32 mannosamine, the 16 mannosamines-NBD-PG-G4-dendrimer was chosen to conjugate TAA for added functionality. Docking results showed that the majority of TAA-conjugated NBD-PG-G4-dendrimer demonstrated a favorable interaction with mannosamine binding site on MR1, thus constituting a promising tool for the targeted delivery of TAA.

Our *in silico* approach effectively narrows down the selection of the best candidates for the synthesis of functionalized PG-dendrimers with desired functionalities. The results of this study will significantly reduce the time and efforts required to experimentally obtain modified dendrimers for optimal controlled delivery of antigens to targeted DC.

ABBREVIATIONS

PG - poly (glutamic acid)

TAA - tumor associated antigens

MR1 - mannose receptor

NBD - nitrobenzoxadiazole

DC - dendritic cells

MAA - melanoma associated antigens

APC - antigen presenting cells

MD - molecular dynamics

NPT - normal pressure and temperature

G4 - generation 4

MHC – Major Histocompatibility Complex

FMOT - Frontier Molecular Orbital Theory

HOMO - Highest Occupied Molecular Orbital

LUMO - Lowest Energy Unoccupied Molecular Orbital

INTRODUCTION

Cancer is one of the leading causes of death worldwide. Metastatic melanoma is the most dangerous type of skin cancer and new treatments are needed due to the development of resistance to most of the available radiotherapy and chemotherapy regimens currently in use [1, 2]. Cancer cells have the ability to develop distinct tactics to evade host immune system, and thus tumor-associated antigens (TAA) recognition by T lymphocytes has led to the development of new strategies to strength tumor specific immune responses [3]. The TAA recognition, internalization and presentation by dendritic cells (DC) to $CD8^+$-T cells and $CD4^+$T-Helper cells specific for tumor epitopes can be induced by an effective cancer vaccine [4]. Among the specific melanoma associated antigens (MAA), MART-1 (or Melan-A) and gp100:209-217 are two highly immunogenic epitopes, presented by major histocompatibility complex (MHC) class I, and frequently recognized by tumor-infiltrating lymphocytes (TIL). Additionally, gp100:44-59, a MHC class II restricted MAA, has also been used to test the effects of MHC class I and class II peptides co-presentation in the induction of antigen-specific anti-tumor immune response [5, 6]. Studies have shown that the combination of MHC class I and II epitopes derived from the same tumor antigen, potentiate anti-tumor effect and long-term tumor-specific immunity [7].

Dendrimers are emerging as a new exciting class of potential delivery systems for anticancer agents or vaccines for the treatment of solid malignancies [8]. Dendrimers are spherical macromolecules with three-domain architecture, consisting of a core, branches and terminal end groups. Variation in synthetic methods and starting materials can result in a wide range of structures with controlled branching, being as well versatile in the nature of terminal groups [9, 10]. The physicochemical features of these molecules are unique because of their low viscosity, molecular topology, overall size

(2 to 10 nm), molecular density and the multiplicity of end groups that can be chemically functionalized [9, 11].

Due to their proper nanoarchitecture, biocompatibility and biodegradability profiles, peptide dendrimers are promising drug delivery systems [12]. They are built using natural amino acids and can be synthesized either by linear combinations of amino acids assembled at a branching point or by using amino acids as focal branching points themselves (e.g. glutamic acid, lysine, and aspartic acid) [13]. A particular characteristic of peptide dendrimer is its asymmetric arrangement, which create different local microenvironments to bind different molecules (drugs, metals or probes) [9].

The functionalization of dendrimers allows the active targeting of antigen presenting cells (APC) and consequently the delivery of immune modulator compounds to different immune cells. APC, namely DC, have a multiplicity of surface receptors (such as MR1) that are involved in the recognition and internalization processes [5].

An appropriate design of dendrimer conjugates could enable the targeting of a specific receptor. Due to its structural complexity, diversity and high degree of chemical space, the prediction and rationalization of the 3D structure of dendrimers is difficult. To overcome these drawbacks, various degrees of complexity from coarse-grained to full atom simulations have been used, namely molecular dynamics (MD) simulations. MD allows understanding the interaction process of dendrimers with drugs and biomolecules at the atomistic level.

This work reports a rational approach to design multifunctional poly (glutamic acid) (PG)-dendrimers with a high potential to target DC and co-deliver antigens and adjuvants simultaneously for a coordinated activation of these APC and consequent

expansion of T cells. Namely, the conjugation of mannosamine to peptidic dendrimers would promote specific interactions with MR1 receptor to enable the targeted delivery of one TAA (MART-1, gp100:44–59 (hereafter gp100:44) and gp100:209–217 (hereafter gp100:209). These multifunctional dendrimers will target relevant cells, but are also expected to modulate cancer antigen intracellular trafficking pathway within the cytoplasm to enhance the selectivity and effectiveness of antitumor immunotherapeutic effect. To monitor the distribution of the dendrimer, nitrobenzoxadiazole (NBD) fluorophore was incorporated in its core, forming NBD-PG-G4-dendrimer that can be further subjected to surface modifications. The main goal of this study was to evaluate *in silico* the effects of NBD-PG-G4-dendrimer surface modifications by mannosamine and TAA, on their intermolecular interactions and potential for targeted delivery. This computer aided molecular design allowed the identification of most suitable candidates for the synthesis of a multifunctional dendrimer with optimal targeted delivery of TAA to DC.

METHODS

Generation of 3D structures of NBD-PG-G4-dendrimer as well as mannosamine and three TAA (MART-1, gp100:44 and gp100:209)

The NBD-PG-G4-dendrimer structures were generated using X-PLOR, as previously described by Martinho *et al* [13]. Mannosamine was built using Maestro software. TAA sequences (Table 1) were obtained in [14, 15, 16] and their 3D structures were generated by peptide structure prediction using PEP-FOLD web server [17]. All structures were saved in *.mae and *.pdb format.

Table 1: Peptide sequence of tumor-associated antigens (TAA)

TAA	Sequence (aa)
MART-1	EAAGIGILTV
gp100:209 - 217	IMDQVPFSV
gp100:44 - 59	WNRQLYPEWTEAQRLD

Molecular Dynamics simulation of NBD-PG-G4-dendrimer, mannosamine and TAA

Mannosamine, TAA and NBD-PG-G4-dendrimer structures were imported to Maestro 2016-2 and then subjected to Protein Preparation Wizard to adjust the protonation states of ionizable groups for pH 7 [18].

Hereafter, all structures were prepared for MD simulations using Desmond. The systems were built using the SPC solvation model and the size of the cubic box was determined automatically by creating a 10 Å (NBD-PG-G4-dendrimer) or 15 Å (mannosamine and TAA) buffer zone around the structures. Appropriate number of ions (Na^+) was added to neutralize the system with further addition of 150 mM NaCl salt.

The MD simulation, structure minimization and relaxation steps were performed for 10 ns (mannosamine and NBD-PG-G4-dendrimer) or 20 ns (TAA) at 300K and 1.03 bar using NPT.

Determination of electronic properties by semi-empirical methods

The electronic properties of the dendrimers were determined by semi-empirical methods using Mopac 2012 [19]. Input files for Mopac (*.mop) were created using Avogadro 2 software [20] and selecting single point energy calculation (for TAA and NBD-PG-G4-dendrimer) or geometry optimization (for mannosamine). The keywords

used were PM7, GRAPHF, MOZYME, NSPA=60, and EPS=78.4. The correct charge state of systems was calculated using Vega ZZ 3.0.5.12 and used in conjunction with the keyword CHARGE. The position of HOMO and LUMO orbitals of all structures were visualized using Jmol 11.2.14 software [21]. Additionally, calculation of ionization potential (I = (HOMO−1) − HOMO), electronic affinity (A = HOMO − LUMO) and the global reactivity indexes: chemical potential (μ = −1/2 (I + A)), electronegativity (χ = −μ), hardness (η =-1/2 (I − A)), softness (S = 1/η) and electrophilicity (ω = χ^2/ 2η).

Docking of mannosamine and TAA to NBD-PG-G4-dendrimer

Docking studies of mannosamine and TAA to NBD-PG-G4-dendrimer to MR1, were performed using HEX 8.0.0 software [22]. The 3D structures of MR1 were obtained in RCSB Protein Data Bank [23], and by homology modelling using Swiss-Model online webserver. The total energy of interactions was calculated based on shape and electrostatics as correlation types followed by OPLS post processing minimization. Saved files of 20 docking poses were visualized in Maestro 2016-2.

Conjugation of mannosamine and TAA to NBD-PG-G4-dendrimer and respective analysis

Mannosamine and TAA amino groups where the LUMO were located were conjugated to carboxylic groups of NBD-PG-G4-dendrimers where HOMO was located, using Maestro 2016-2 software. Firstly, 1, 16 and 32 mannosamines or 1, 5 and 10 TAA, individually, were conjugated to NBD-PG-G4-dendrimer. Secondly, 16 mannosamines were conjugated to NBD-PG-G4-dendrimer structure, which was further used to conjugate 2 or 4 TAA.

For all conjugated structures, MD simulations were performed using fully solvated systems that were built using SPC solvation model, 10 Å as the size of the cubic box around the conjugated structures with addition of ions (Na^+) and 150 mM NaCl salt. The MD simulations that followed initial structure minimization and relaxation steps were performed for 1ns at 300K and 1.03 bar.

The determination of electronic properties and the docking studies of the mannosamine or TAA NBD-PG-G4-dendrimer conjugates and TAA 16 Mannosamine-NBD-PG-G4-dendrimer were performed as described above.

RESULTS and DISCUSSION

Computational modeling and MD are valuable tools for the design and optimization of drug candidates and polymeric structures. Thus, there is a growing interest in applying computational chemistry tools to study dendrimers. Molecular modeling of dendrimers offers a means to study conformation and different features of the dynamic behavior of dendrimers, on the atomistic level, that are difficult to probe experimentally. Thereafter, these approaches allow the elucidation of some of the key interactions of functionalized dendrimers with therapeutic molecules and biological systems, such as proteins and receptors as well as with lipid membranes.

As a result, our *in silico* strategy was employed to understand the impact of the surface modification of dendrimers, with distinct numbers of TAA and mannosamine molecules, on their conformation and dynamic interactions with target receptors.

*Generation of 3D structures: NBD-PG-G4-dendrimer, mannosamine and TAA (MART-1, gp100:44 and gp100:209)*

The three-dimensional structures of NBD-PG-G4-dendrimer, as well as mannosamine and three different TAA (MART-1, gp100:44 and gp100:209) were generated. The generation 4 (G4) of PG dendrimer has 64 carboxylic end groups (32 on the backbone chain and 32 on the side chains) available for covalent interaction with mannosamine and/or TAA. Additionally, incorporation of NBD (a fluorophore) in the core, aimed to follow the dendrimer delivery in the biological studies, was optimal at PG G4 dendrimer. Under these conditions, NBD would not be exposed to the surface thus resulting in NBD-PG-G4-dendrimers as the core for further surface modifications. We predicted that the fluorophore was fully incorporated in the core of the dendrimer, thus not forming undesired intermolecular interactions with other molecules or targets [13]. The predicted structures of TAA on their own, resembled some of their structural features in experimentally-determined complexes with MHC class I biopolymers, i.e. MART-1 complexed with HLA-A2 found in the Protein Data Bank entry 3MRO. Therefore, these predicted structures were further used in the conjugation studies.

The resulting structures were submitted to MD simulations, using the conditions previously described in Methods. In each trajectory of MD simulation, 1000 different structures were saved and clustered to select the best representative structures for the conjugation studies. Moreover, analysis of all trajectory profile allowed the study of conformational dynamic structures of NBD-PG-G4-dendrimer, as well as of all TAA, individually.

Calculation of electronic properties of NBD-PG-G4-dendrimer, mannosamine and TAA (MART-1, gp100:44 and gp100:209), individually and conjugated

The Frontier Molecular Orbital Theory (FMOT) hypothesize that the interaction between the HOMO and the LUMO orbitals of molecules undergoing a reaction, can provide a good approximation of reaction outcome [24]. The reaction occurs with increasing and possible overlap of HOMO and LUMO orbitals. Results demonstrated that HOMO molecular orbitals of the dendrimer were located on the carboxylic acid groups from backbone chain and it could preferentially interact with LUMO molecular orbitals of amine group from mannosamine or TAA, as shown in Figure 1A. These results are in agreement with a previous study performed by our group, where HOMO of a generation 3.5 PAMAM is located on one of the terminal carboxylic acid groups [25]. Moreover, HOMO and HOMO-1 orbitals are located at the end groups of the branches of the dendrimer, being this position favorable for further conjugations. The calculations of HOMO and LUMO orbital energies enabled the prediction of the next conjugation sites on dendrimer for additional molecules, such as mannosamine and TAA (Figure 1B and C, respectively). We chose the most representative conformation per analogue for the calculation of the electronic properties, having in consideration the time required for these electronic calculations, the demand for computational resources and the information that most probably will be obtained.

The conjugation of NBD-PG-G4-dendrimer with different molar ratios of mannosamine and each TAA was performed. NBD-PG-G4-dendrimer was conjugated with 1, 16 and 32 mannosamines, and separately with 1, 5 and 10 individual TAA. The addition of the first mannosamine or TAA is favorable because the HOMO is located on the surface carboxylic group and exposed for reaction (Figure 1D).
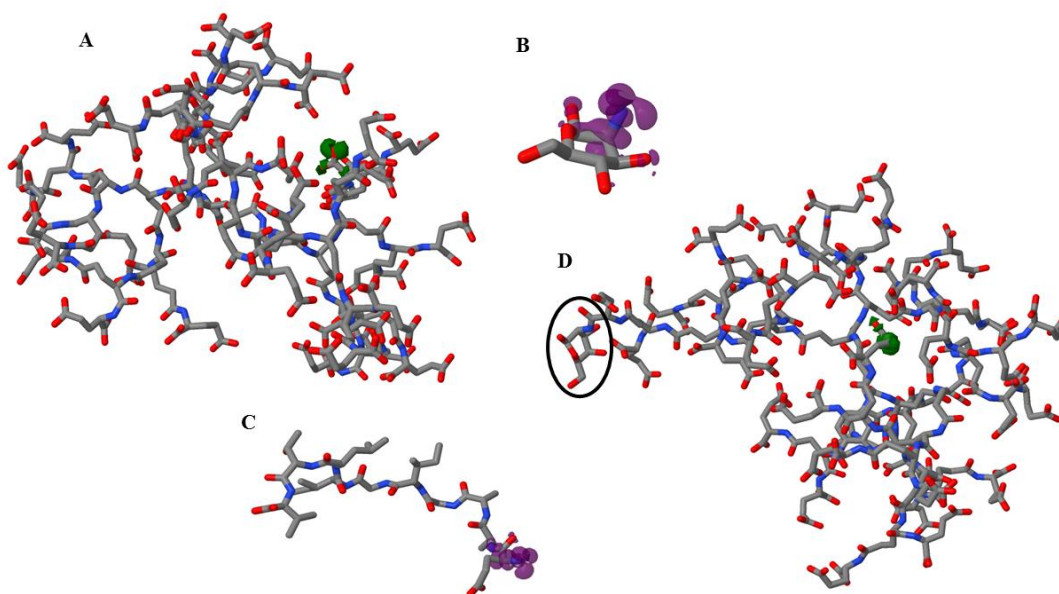
Figure 1 – Representative HOMO and LUMO orbitals of NBD-PG-G4-dendrimer (green) (A), mannosamine (purple) (B), MART-1 (purple) (C) and mannosamine-conjugated to NBD-PG-G4-dendrimer (green) (D). In D, the HOMO and LUMO orbitals of mannosamine conjugated to NBD-PG-G4-dendrimer are placed in the opposite side of the first mannosamine connected to dendrimer (black circle).

Then, the difference in energies between HOMO of dendrimer and LUMO of mannosamine / TAA for subsequent additions was determined and analyzed. The obtained results showed no significant differences in the gap energy of HOMO/LUMO for all NBD-PG-G4 dendrimer conjugates, despite the increase in size and number of occupied carboxylic groups (Table 2). These results could suggest a similar reactivity of the dendrimer for the conjugation of mannosamine and TAA regardless of number of modified terminal carboxylic groups.

Table 2 also shows the values of the calculated global chemical reactivity parameters for the conjugation of NBD-PG-G4-dendrimer to 1, 16 and 32 mannosamines, and separately to 1, 5 and 10 individual TAA. The ionization potential values increased

with the augment of mannosamine molecules linked to NBD-PG-G4-dendrimer, while for the conjugation of TAA, the values maintained unchanged. The electronic affinity values were lower in NBD-PG-G4-dendrimers conjugated with higher number of mannosamines (from 1 to 32). Again, these values remained unchanged despite the number of TAA conjugated to the NBD-PG-G4-dendrimer. No differences were observed in the values of global reactivity indexes (chemical potential, electronegativity, hardness, softness and electrophilicity) obtained for the conjugation of NBD-PG-G4-dendrimer to 1 and 16 mannosamines, and separately to 1, 5 and 10 individual TAA. However, there was a notable change in value of hardness from -3.03 to -3.55 for the NBD-PG-G4-dendrimer conjugated with 32 mannosamines.

FMOT also hypothesized that smaller gaps among HOMO and LUMO may lead to higher probability for the reaction [24]. Having in consideration the size of mannosamine, the results suggest that this molecule could occupy all 64 binding sites of the NBD-PG-G4-dendrimer. The similar trend would be expected for TAA, however, due to the size of the peptides, the complete conjugation is unlikely to occur due to steric hindrance by those already conjugated peptides. However, our results demonstrated that the amine group of mannosamine and each TAA bound preferentially to the carboxylic group of the backbone chain, instead of the carboxylic group on side chains. Therefore, only 32 terminal groups can be expected to act as acceptors for conjugations by mannosamine, as there is a notable change in hardness, thus indicating that further conjugation with mannosamine may be precluded.

Table 2 – Values of the highest occupied molecular orbital (HOMO) energy determined for NBD-PG-G4-dendrimer (and its conjugated form) and the lowest unoccupied molecular orbital (LUMO) of mannosamine (0.68 eV). MART-1 (0.16 eV). gp100:209 (-0.25 eV) or gp100:44 (-0.34 eV), according with used in conjugated structure. Additionally, vibrational analyses were performed, namely ionization potential and the electronic affinity calculations. The global reactivity indexes specifically chemical potential, electronegativity, hardness, softness and electrophilicity calculations were also carried out.

Structure	HOMO (eV)	HOMO - 1 (eV)	LUMO (eV)	HOMO - LUMO* gap (eV)	Ionization potential (I)	Electronic affinity (A)	Chemical potential (μ)	Electronegativity (χ)	Hardness (η)	Softness (S)	Electrophilicity (ω)
Mannosamine	-10.70	-11.29	0.68	-	-0.59	-11.38	5.98	-5.98	-5,40	-0,19	-3,32
MART-1	-9.52	-9.95	0.16	-	-0.43	-9.68	5.05	-5.05	-4,63	-0,22	-2,76
gp100:209	-8.90	-9.48	-0.25	-	-0.58	-8.65	4.61	-4.61	-4,04	-0,25	-2,64
gp100:44	-8.48	-8.60	-0.34	-	-0.12	-8.14	4.13	-4.13	-4,01	-0,25	-2,13
NBD-PG-G4-dendrimer : mannosamine	-7.99	-8.47	-2.04	8.77	-0.48	-5.95	2.88	-2.88	-2,74	-0,37	-1,89
NBD-PG-G4-dendrimer : mannosamine (1:1)	-7.50	-7.79	-2.06	8.18	-0,29	-5.44	3.34	-3.34	-2,58	-0,39	-1,59
NBD-PG-G4-dendrimer : mannosamine (1:16)	-8.58	-8.74	-2.36	9.26	-0,16	-6.22	3.32	-3.32	-3,03	-0,33	-1,68
NBD-PG-G4-dendrimer : mannosamine (1:32)	-8.96	-8.99	-1.83	9.64	-0,03	-7.13	3.14	-3.14	-3,55	-0,28	-1,81
NBD-PG-G4-dendrimer : MART-1 (1:1)	-8.06	-8.12	-2.13	8.22	-0,06	-5.93	2.97	-2.97	-2,94	-0,34	-1,53
NBD-PG-G4-dendrimer : MART-1 (1:5)	-8.15	-8.08	-2.27	8.31	0,07	-5.88	2.90	-2.90	-2,98	-0,34	-1,42

NBD-PG-G4-dendrimer : MART-1 (1:10)	-8.79	-8.80	-1.96	8.95	-0,01	-6.83	3.42	-3.42	-3,41	-0,29	-1,72
NBD-PG-G4-dendrimer : gp100:209 (1:1)	-7.98	-8.19	-2.09	7.73	-0,21	-5.89	3.05	-3.05	-2,84	-0,35	-1,64
NBD-PG-G4-dendrimer : gp100:209 (1:5)	-8.04	-8.16	-2.35	7.79	-0,12	-5.69	2.90	-2.90	-2,79	-0,36	-1,52
NBD-PG-G4-dendrimer : gp100:209 (1:10)	-7.80	-7.94	-2.35	7.55	-0,14	-5.45	2.80	-2.80	-2,66	-0,38	-1,47
NBD-PG-G4-dendrimer : gp100:44 (1:1)	-7.87	-7.88	-2.32	7.53	-0,01	-5.55	2.78	-2.78	-2,77	-0,36	-1,40
NBD-PG-G4-dendrimer : gp100:44 (1:5)	-7.91	-7.95	-2.46	7.57	-0,04	-5.45	2.74	-2.74	-2,71	-0,37	-1,39
NBD-PG-G4-dendrimer : gp100:44 (1:10)	-7.77	-7.85	-2.53	7.43	-0,08	-5.24	2.66	-2.66	-2,58	-0,39	-1,37

Docking studies – mannose receptor (MR1) and mannosamine or TAA conjugated to NBD-PG-G4-dendrimer

Docking studies should predict the best orientation of a structure to another structure, or corresponding receptor, to form a more stable complex. MR1 has an extracellular portion constituted by various C-type carbohydrate recognition domains that allow recognition of a diverse range of glycoconjugate ligands [26]. As result, MR1, which is present in macrophages and DC, plays a central role in the coordination of innate and adaptive immune responses through the increase of uptake and consequent processing of soluble glycoconjugates released from pathogens [23].

Mannosamine is the principal ligand that binds to MR1 receptor. The augment on mannosamine in the dendrimeric structure could potentiate the interaction with MR1 receptor and facilitate intracellular trafficking and processing. The structure of MR1 (1EGI) was obtained in Protein Data Bank. However, due to the poor definition of the active site responsible for the mannosamine binding and consequently obtained poor docking results, a new 3D structure of MR1 was generated by homology modelling. This resulted in a model generated by Swiss-Model server in automated mode based on the 1EGI structure, as a template. All docking studies were performed using the model 2 that had well defined mannosamine binding site in a good agreement with previously identified residues [23] and hereafter referred only as MR1.

Obtained results from docking analysis showed that mannosamine (Figure 2A) alone interacted with the residues that define receptor MR1 binding site, constituted by amino acids glutamic acid (position 743) and asparagine (positions 745 and 746), as previously observed by Feinberg *et al* [23]. The TAA had preferential interactions with other surfaces on the MR1, without any selectivity. Furthermore, all tested

mannosamine and TAA conjugated to NBD-PG-G4-dendrimer bound to the MR1 receptor, showing similar profiles. Notably, increasing the number of mannosamine conjugated to NBD-PG-G4-dendrimer (from 16 to 32 mannosamines), the conjugates formed more favorable interactions with mannosamine binding site, as showed in Figures 2B and 2C, respectively. This effect could be justified by the balanced charge of total dendrimer and changed conformations with higher loadings of mannosamine.

Although 32 mannosamine-linked NBD-PG-G4-dendrimer had better docking profile compared with 16 mannosamine-linked NBD-PG-G4-dendrimer, it was found that the LUMO of dendrimer conjugated with 32 mannosamines was not located on the carboxylic group at the glutamic acid side chain, and therefore, according to FMOT, further conjugation of TAA is not likely to occur. Due to these constrains in 32 mannosamine-linked NBD-PG-G4-dendrimer, the 16 mannosamine-linked NBD-PG-G4-dendrimer structure was selected as a candidate for further conjugation with two and four TAA.
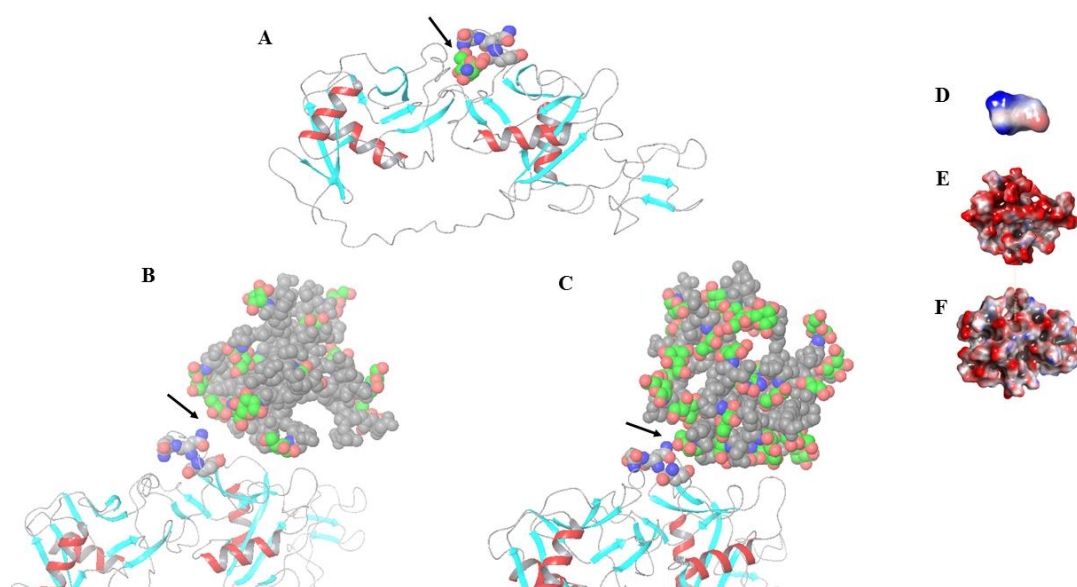
Figure 2 – Docking conformations of mannosamine (green, red and blue structure) (A), 16 mannosamine conjugated to NBD-PG-G4-dendrimer (grey, green, red and blue structure) (B) and 32 mannosamine conjugated to NBD-PG-G4-dendrimer (grey, green, red and blue structure) (C) to the core of mannose receptor, MR1, represented by three amino acids: Glutamic acid (position 743), aspartame (position 745 and 746) (grey, blue and red). D, E and F show the electrostatic surface representations of mannosamine, and 16 and 32 mannosamines conjugated to NBD-PG-G4-dendrimer, respectively. In A, mannosamine is directly docked in the core of MR1. In B, 16 mannosamine conjugated to NBD-PG-G4-dendrimer are not so close to the receptor core when compared with 32 mannosamine conjugated to NBD-PG-G4-dendrimer (C).

Conjugation of TAA to 16 mannosamine-linked NBD-PG-G4-dendrimer and respective analysis (molecular dynamics simulation and docking)

The combination of different TAA with mannosamine-linked NBD-PG-G4-dendrimer could potentiate the targeted immune response. Due to possible steric constrains that could arise from the conjugation of high number of TAA, the conjugation of only two and four TAA to 16 mannosamine-linked NBD-PG-G4-dendrimer was explored.

The conjugation of the first TAA (MART-1, gp100:44 and gp100:209) was performed according to the obtained HOMO from 16 mannosamine-linked NBD-PG-G4-dendrimer. The conjugation sites are localized on the carboxylic acid groups from backbone chain of 16 mannosamine-linked NBD-PG-G4-dendrimer, similarly to the previously described conjugation sites for NBD-PG-G4-dendrimer.

MD simulations were performed during 1 and 10 ns for 4 TAA connected to 16 mannosamine-linked NBD-PG-G4-dendrimer, however no major differences were

observed. HOMO for higher number conjugations (2, 3 and 4 TAA) were localized on the carboxylic groups close to first conjugations site, thus leaving mannosamine rich surface available to interact with MR1 and promote the targeted delivery of the multifunctional dendrimer (Figure 3).
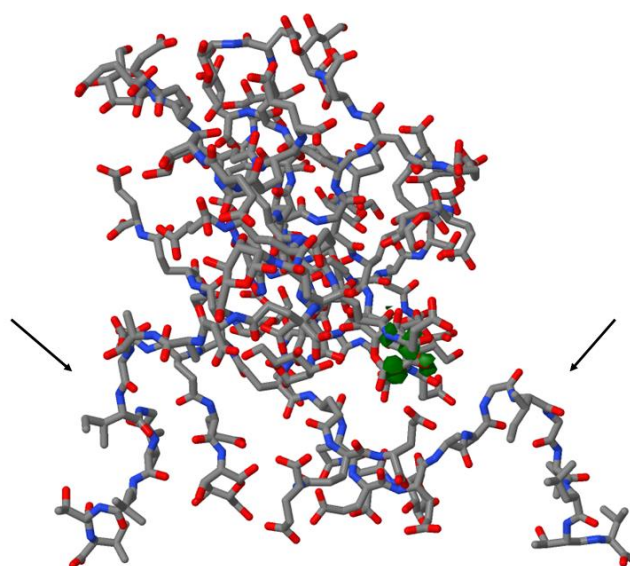
Figure 3: Representative HOMO and LUMO orbitals of two MART-1 linked to 16 mannosamine – NBD-PG-G4-dendrimer (green). The HOMO and LUMO orbitals of TAA- 16 mannosamine conjugated to dendrimer are placed in COOH groups of the closer branches to TAA instead of opposite side of MART-1 position. Arrows show the MART-1 positions.

Docking studies of multifunctional dendrimers with increasing number of TAA conjugated to 16 mannosamine-linked NBD-PG-G4-dendrimer resulted in higher likelihood of sugar moiety on the dendrimer surface to interact with mannosamine binding site on the MR1 receptor. Thus, 4 TAA associated to 16 mannosamine-linked NBD-PG-G4-dendrimer were the conjugates that presented a better docking profile.

Among these results, MART-1 associated to 16 mannosamine-linked NBD-PG-G4-dendrimer did not show a favorable interaction with the binding site on the MR1 (Figure 4A), compared with 4 gp100:44 or gp100:209 associated to 16 mannosamine-linked NBD-PG-G4-dendrimer (Figure 4 B). Therefore, MART-1 is not a good TAA to be conjugated with 16 mannosamine-linked NBD-PG-G4-dendrimer, which most likely result from the preferential non-specific interactions with MR1 that would not warrant the targeted delivery utilizing mannosamine on the dendrimer surface.
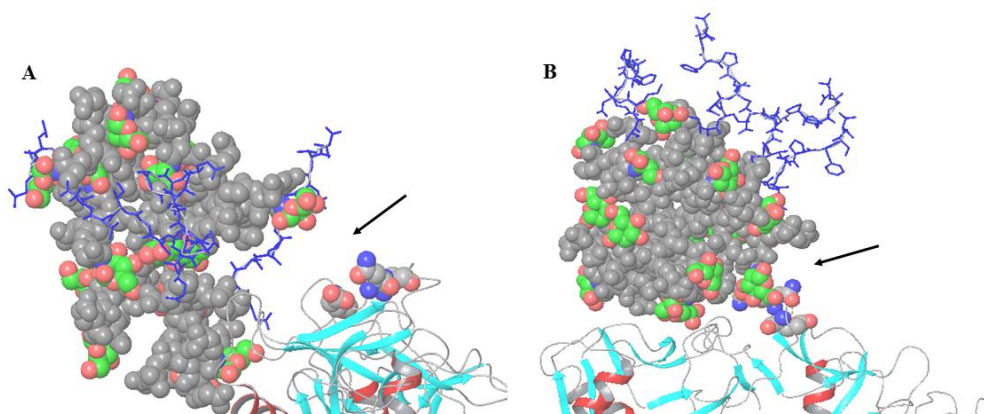
Figure 4: Docking conformations of TAA (blue) linked to 16 mannosamine-conjugated NBD-PG-G4-dendrimer (grey, green and red structure) and bound to the core of mannose receptor, MR1, represented by three amino acids: glutamic acid (position 743), aspartame (position 745 and 746) (grey, blue and red). In A) MART-1 linked to 16 mannosamine conjugated to NBD-PG-G4-dendrimer is further away from the core of MR1, compared with gp100:209 (B) or gp100:44 (not shown) linked to 16 mannosamine-conjugated NBD-PG-G4-dendrimer that are closer to the amino acids of the core of MR1.

Therefore, these *in silico* studies suggest that most likely candidates that would have viable synthetic route and favorable interaction profile with MR1 to achieve targeted delivery of TAA to DC are: gp100:44 or gp100:209 conjugated to 16 mannosamine-linked NBD-PG-G4-dendrimers.

CONCLUSIONS

Understanding molecular interactions is fundamental to improve targeted delivery systems. The MD, docking studies and calculation of electronic properties performed for mannosamine, TAA and all conjugated forms provided an *in silico* tool for the design of multifunctional dendrimers and assessment of their potential for targeted delivery. Particularly, docking studies can offer greater insight on the interaction of dendrimers with bioactive molecules and biological targets. The optimal design of a dendrimer with a modified core and functionalized surface allows monitoring their cellular uptake without affecting the desired biological activity. Additionally, a targeted delivery of TAA will increase their uptake and processing, favoring an extensive presentation of the epitope to T cells.

This approach suggested candidates for full mechanistic studies on a reduced set of molecules with optimized properties. Important results were obtained, namely showing that mannosamine had no steric impediment to connect to 64 carboxylic groups on the surface of NBD-PG-G4-dendrimer. Additionally, electronic studies from MD simulation showed that the carboxylic acid groups on the backbone chain are the preferred site for chemical conjugation when compared to the carboxylic group of the side chain, thus suggesting a reduced likelihood to achieve full conjugation of all 64 terminal carboxylic groups. It was also verified by electronic studies that reactivities of

mannosamine and TAA to connect to dendrimeric structures are similar. However due to the steric hindrance, TAA may not have the same conjugation efficiency, which would prevent their successful conjugation to all surface carboxylic groups.

Differences in docking of dendrimer structures to MR1 receptor were observed. Despite that the 32 mannosamines conjugated to NBD-PG-G4-dendrimer showed the best interaction profile with MR1, lack of availability of the carboxylic acid groups on the backbone chain suggested that this is not a good candidate for further conjugation of TAA.

Therefore, the NBD-PG-G4-dendrimer conjugated with 16 mannosamines was chosen as a platform to further bind TAA. It was observed that after conjugating first TAA on the 16 mannosamine NBD-PG-G4-dendrimer, the conjugation sites for subsequent TAA conjugation were situated in a close proximity. This creates the opportunity to have TAA rich surfaces on one side of the dendrimer, while leaving the mannosamines on the opposite side free for favorable interactions with MR1.

This thorough study thus allowed the selection of the best candidates for future experimental work focused on the development of a cancer vaccine, through the synthesis of a lower number of PG G4 dendrimer conjugates to achieve an optimal system for targeted delivery of TAA.

DISCLOSURE OF INTEREST

REFERENCES

1.   Nikolaou V, Stratigos AJ. Emerging trends in the epidemiology of melanoma. The British journal of dermatology. 2014;170:11-9.

2.   Huang YY, Vecchio D, Avci P, Yin R, Garcia-Diaz M, Hamblin MR. Melanoma resistance to photodynamic therapy: new insights. Biological chemistry. 2013;394:239-50.

3.   Lu Y, Kawakami S, Yamashita F, Hashida M. Development of an antigen-presenting cell-targeted DNA vaccine against melanoma by mannosylated liposomes. Biomaterials. 2007;28:3255-62.

4.   Rosenberg SA. Progress in human tumour immunology and immunotherapy. Nature. 2001;411:380-4.

5.   Silva JM, Zupancic E, Vandermeulen G, Oliveira VG, Salgado A, Videira M, Gaspar M, Graca L, Preat V, Florindo HF. In vivo delivery of peptides and Toll-like receptor ligands by mannose-functionalized polymeric nanoparticles induces prophylactic and therapeutic anti-tumor immune responses in a melanoma model.

Journal of controlled release : official journal of the Controlled Release Society. 2015;198:91-103.

6.	Benlalam H, Labarrière N, Linard B, Derré L, Diez E, Pandolfino MC, Bonneville M, F. J. Comprehensive analysis of the frequency of recognition of melanoma associated antigen (MAA) by CD8 melanoma infiltrating lymphocytes (TIL): implications for immunotherapy. Eur J Immunol. 2001;31:2007-15.

7.	Touloukian CE, Leitner WW, Topalian SL, Li YF, Robbins PF, Rosenberg SA, NP R. Identification of a MHC Class II-Restricted Human gp100 Epitope Using DR4-IE Transgenic Mice J Immunol. 2000;164:3535-42.

8.	Menjoge AR, Kannan RM, Tomalia DA. Dendrimer-based drug and imaging conjugates: design considerations for nanomedical applications. Drug discovery today. 2010;15:171-85.

9.	Kesharwani P, Jain K, Jain NK. Dendrimer as nanocarrier for drug delivery. Progress in Polymer Science. 2014;39:268–307.

10.	Heegaard PM, Boas U, Sorensen NS. Dendrimers for vaccine and immunostimulatory uses. A review. Bioconjugate chemistry. 2010;21:405-18.

11.	Hsu HJ, Bugno J, Lee SR, Hong S. Dendrimer-based nanocarriers: a versatile platform for drug delivery. Wiley interdisciplinary reviews Nanomedicine and nanobiotechnology. 2017;9.

12.	Pu Y, Chang S, Yuan H, Wang G, He B, Gu Z. The anti-tumor efficiency of poly(L-glutamic acid) dendrimers with polyhedral oligomeric silsesquioxane cores. Biomaterials. 2013;34:3658-66.

13.	Martinho N, Silva L, Florindo H, Brocchini S, Zloh M, Barata TS. Rational design of novel fluorescent tagged glutamic acid dendrimers with different terminal

groups and in-silico analysis of their properties International Journal of Nanomedicine. 2017;Under review.

14.   Lofus DJ, Castelli C, Clay TM, Squarcina, Marincola FM, Nishimura V, Parmiani G, Appella E, L R. Identification of Epitope Mimics Recognized by CTL Reactive to the Melanoma/Melanocyte-derived Peptide MART-l(27_35) JEM 184 (2): 647. 1996;184:647-57.

15.   Fonteneau J, Larssona M, Somersana S, Sandersa C, Münza C, Kwokb WW, Bhardwaja N, Jotereauc F. Generation of high quantities of viral and tumor-specific human CD4+ and CD8+ T-cell clones using peptide pulsed mature dendritic cells. Journal of Immunological Methods. 2001;258:11-126.

16.   Lee K, Panelli M, Kim C, Riker A, Bettinotti M, Roden M, Fetsch P, Abati A, Rosenberg S, Marincola F. Functional Dissociation Between Local and Systemic Immune Response During Anti-Melanoma Peptide Vaccination. J Immunol. 1998;161:4183-94.

17.   Shen Y, Maupetit J, Derreumaux P, Tufféry P. Improved PEP-FOLD approach for peptide and miniprotein structure prediction. Journal of chemical theory and computation. 2014;10:4745-58.

18.   Osguthorpe D, Sherman W, Hagler A. Exploring Protein Flexibility: Incorporating Structural Ensembles From Crystal Structures and Simulation into Virtual Screening Protocols. J Phys Chem B. 2012;116:6952–9.

19.   Stewart JJ. Mopac2012. Stewart Computational Chemistry, Colorado Springs, CO, USA. 2012.

20.   Hanwell MD, Curtis DE, Lonie DC, Vandermeersch T, Zurek E, Hutchison GR. Avogadro: an advanced semantic chemical editor, visualization, and analysis platform. Journal of cheminformatics. 2012;4:17.

21.   Cass ME, Rzepa HS, Rzepa DR, Williams CK. The use of the free, open-source program Jmol to generate an interactive web site to teach molecular symmetry. J Chem Educ. 2005;82:1736.

22.   Ritchie D, Orpailleur T. Hex 8.0. 0 User Manual. 1996.

23.   Feinberg H, Park-Snyder S, Kolatkar AR, Heise CT, Taylor ME, Weis WI. Structure of a C-type carbohydrate recognition domain from the macrophage mannose receptor. The Journal of biological chemistry. 2000;275:21539-48.

24.   K. F. Role of frontier orbitals in chemical reactions. Science. 1982;218:747-54.

25.   Barata TS, Brocchini S, Teo I, Shaunak S, M. Z. From sequence to 3D structure of hyperbranched molecules: application to surface modified PAMAM dendrimers. J Mol Model. 2011;17:2741-9.

26.   Catherine E. Napper MHD, and Maureen E. Taylor§. An Extended Conformation of the Macrophage Mannose Receptor. Journal of Biological Chemistry. 2001;276:14759–66.